5ICEGE
5th International Conference on Earthquake Geotechnical Engineering
January 2011, 10-13 | Santiago, Chile
Paper No. EOFGR

EVALUATION OF VARIOUS DEFINITIONS OF CHARACTERISTIC PERIOD OF EARTHQUAKE GROUND MOTIONS

Russell A. GREEN [1], Jongwon LEE[2], Wanda CAMERON [3], and Alfredo ARENAS [4]

ABSTRACT

The objective of the study presented herein is to evaluate various definitions of "characteristic" period of earthquake ground motions for use in the analysis of the dynamic response of soil profiles and retaining walls. The Fourier decomposition of earthquake ground motions shows that they are comprised of a range of frequencies, each having an associated amplitude and phase. However, in engineering practice it is useful to characterize a ground motion by one period, the motion's "characteristic" period. In this study, five commonly used definitions of characteristic period are examined: the mean period (T_m); the average spectral period (T_{avg}); the smoothed spectral period (T_o); the median spectral velocity-acceleration period ($T_{V/A50}$); and the peak ground velocity-acceleration period ($T_{v/a}$). The characteristic period definitions were assessed by computing the amplification of earthquake ground motions propagated up through shallow soil profiles (e.g., backfill of retaining walls) and deeper soil profiles. These results were compared to the analytical solution of sinusoidal motions propagated up through the same soil profiles, where the periods of the sinusoidal motions equaled the characteristic periods of the earthquake ground motions. A validation metric was used to determine which characteristic period definition is most suitable for site response and retaining wall analyses. The results showed that characterizing an earthquake ground motion by a single period, regardless of how quantified, is tenuous. However, of the definitions examined, T_o is the most suitable definition for motions used in the dynamic response of both soil profiles and retaining wall.

Keywords: Characteristic period, Earthquake motions, Site response, Ground motion amplification

INTRODUCTION

The objective of the study presented herein is to evaluate various definitions of "characteristic" period of earthquake ground motions, particularly for motions that will be used in the analysis of the dynamic response of soil profiles and retaining walls. The Fourier decomposition of earthquake ground motions shows that they are comprised of a range of frequencies, each having an associated amplitude and phase. However, engineering analysis/design procedures sometime call for the frequency content of earthquake ground motions to be characterized by a single period (e.g., Shimazaki and Sozen, 1984; Goughnour and Pestana, 1998; Blake et al., 2002; Green and Cameron, 2003; Stewart et al., 2003; Green et al., 2008). Also, the quantification of the frequency content by a single characteristic period often facilitates the

[1] Associate Professor, Charles E. Via, Jr. Department of Civil Engineering, Virginia Tech, Blacksburg, VA, USA, e-mail: rugreen@vt.edu
[2] Assistant Project Engineer Associate, Paul C. Rizzo Associates, Inc., Pittsburgh, PA, USA, e-mail: Jongwon.Lee@rizzoassoc.com
[3] Doctoral Candidate, Department of Civil Engineering, University of Michigan, Ann Arbor, MI, USA, e-mail: wcameron@umich.edu
[4] Doctoral Candidate, Charles E. Via, Jr. Department of Civil Engineering, Virginia Tech, Blacksburg, VA, USA, e-mail: aarenas@vt.edu

selection of ground motion time histories for various types of engineering analyses (e.g., Stewart et al., 2001), with the focus of the study presented herein being on selection of ground motions for analyzing the dynamic response of soil profiles and retaining walls.

Numerous definitions have been proposed for characteristic period. For example, the authors found twenty eight different definitions of characteristic period in literature. In the study presented herein, five of the more commonly used definitions are examined. These include the mean period (T_m), the average spectral period (T_{avg}), the smoothed spectral period (T_o), the median spectral velocity-acceleration period ($T_{V/A50}$), and the peak ground velocity-acceleration period ($T_{v/a}$). Recent ground motion predictive relationships that express these periods as functions of earthquake magnitude (M), site-to-source distance (R), site conditions, etc. are given in Rathje et al. (1998), Rathje et al. (2004), and Lee (2009).

The five definitions of characteristic period were assessed by computing the amplification of earthquake ground motions propagated up through shallow soil profiles (e.g., backfill of retaining walls) and deeper soil profiles. For these analyses, eleven time histories (ten earthquake time histories and one windowed sine wave) and nineteen soil profiles were used, for a total of 209 site response analyses. These results were compared to the analytical solution of infinite duration, sinusoidal motions propagated up through the same soil profiles. For these latter set of computations, the periods of the sinusoidal motions were set equal to the various characteristic periods of the earthquake ground motions. A "validation metric" was then used to determine which characteristic period definition is most suitable for site response and retaining wall analyses. The validation metric is a single number ranging from 0 to 1, indicating that the characteristic period definition is very poor and very good, respectively. The validation metric equation used in this study is a modification of one proposed by Oberkampf and Trucano (2002) for validating numerical models used in computational fluid dynamics, whereby numerical predictions are compared to experimental data, hence the name "validation metric".

In the subsequent sections of this paper, first, a brief review is presented on the five definitions of characteristic period that are assessed in this study. Then, a discussion of the eleven time histories used in this study is presented, to include a listing of the characteristic periods of each motion. This is followed by a presentation of the site response analyses that were performed and the analytical solution. Next, an overview of the validation metric equation is given, and the validation metrics for each characteristic period definition are listed. Finally, a brief discussion is presented on interpreting the validation metrics, and a recommendation is made regarding which characteristic period definition is most suitable for selecting motions for use in site response and retaining wall analyses.

CHARACTERISTIC PERIOD DEFINITIONS

As stated in the Introduction, the authors found twenty eight different definitions of characteristic period in literature, both in engineering seismology and earthquake engineering studies. Herein, five of the more commonly used definitions are examined: the mean period (T_m); the average spectral period (T_{avg}); the smoothed spectral period (T_o); the median spectral velocity-acceleration period ($T_{V/A50}$); and the peak ground velocity-acceleration period ($T_{v/a}$). Rathje et al. (1998), Rathje et al. (2004), and Lee (2009) give detailed reviews of these definitions, to include their origins/previous uses, and present updated ground motion predictive relationships for each. Each of these characteristic period definitions is briefly outlined below.

Mean Period (T_m)

The mean period (T_m) is computed from the Fourier amplitude spectrum of an acceleration time history by the following equation (Rathje et al., 2004):

$$T_m = \frac{\sum_i FA_i^{\,2} \cdot (1/f_i)}{\sum_i FA_i^{\,2}} \quad \text{for } 0.25 \text{ Hz} \le f_i \le 20 \text{ Hz, with } \Delta f \le 0.05 \text{ Hz} \tag{1}$$

where: FA_i is the Fourier amplitude; f_i is the discrete frequency corresponding to the FA_i; and Δf is the frequency interval. Equation 1 yields the weighted average of the period (i.e., $1/f_i$) from 0.05 to 4 sec (or 0.25 to 20 Hz), with the weighting based on the squared Fourier amplitudes. An example of the squared Fourier amplitude spectrum for an earthquake motion and the frequency range over which T_m is computed is shown in Figure 1.

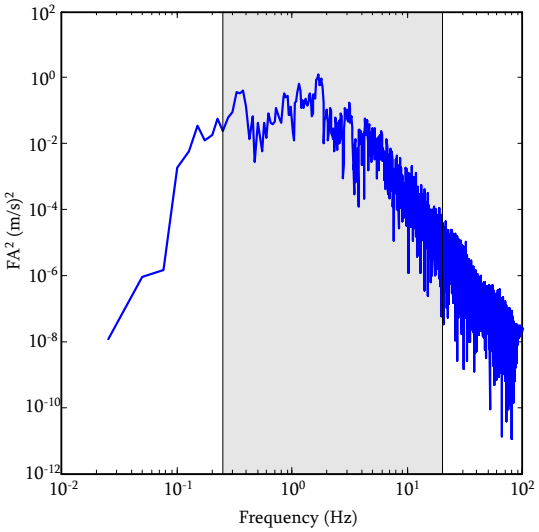

Figure 1. **Example of squared Fourier amplitude and the frequency range considered in computation of T_m (shown in gray background) for an earthquake ground motion (Lee, 2009).**

Average Spectral Period (T_{avg})

Rathje et al. (2004) proposed the average spectral period (T_{avg}), which is computed from the normalized pseudo spectral acceleration response spectrum:

$$T_{avg} = \frac{\sum_i T_i \cdot \left(\frac{PSA(T_i)}{pga} \right)^2}{\sum_i \left(\frac{PSA(T_i)}{pga} \right)^2} \quad \text{for } 0.05 \le T_i \le 4 \text{ sec, with } \Delta T \le 0.05 \text{ sec} \tag{2}$$

where: PSA_i is the 5% damped pseudo spectral acceleration at T_i; T_i is the discrete period of a single degree of freedom oscillator; and ΔT is the period interval. Similar to T_m, T_{avg} is a weighted average of period, with the weighting based on the squared pseudo spectral acceleration amplitude over the period range of 0.05 to 4.0 sec. An example of a normalized pseudo acceleration spectrum along with the period range over which T_{avg} is computed is shown in Figure 2.

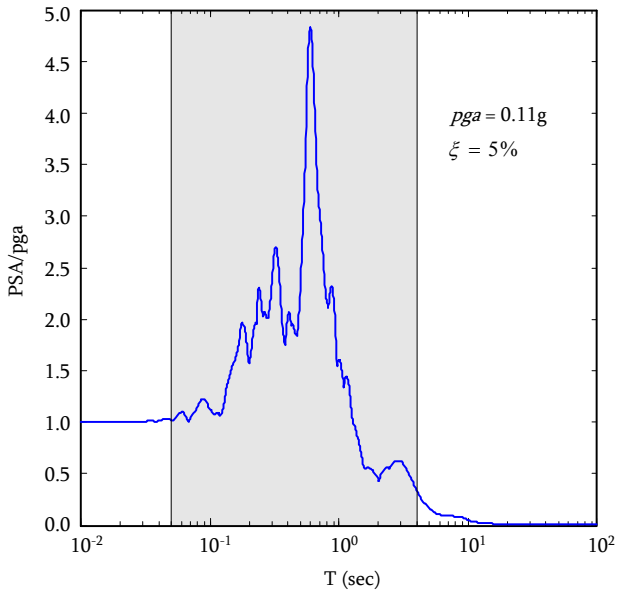

Figure 2. Example of normalized pseudo spectral acceleration spectrum (damping ratio $\xi = 5\%$) and the period range considered in computation of T_{avg} (shown in gray background) for earthquake ground motion (Lee, 2009).

Smoothed Spectral Period (T_o)

Rathje et al. (1998) proposed the smoothed spectral period (T_o), which is determined by using the 5% damped pseudo acceleration spectra normalized by the peak ground acceleration. T_o is defined as:

$$T_0 = \frac{\sum_i T_i \cdot \ln\left(\frac{PSA(T_i)}{pga}\right)}{\sum_i \ln\left(\frac{PSA(T_i)}{pga}\right)} \quad \text{for } T_i \text{ having } PSA/pga \geq 1.2;\ \Delta \log T_i \leq 0.02 \text{ sec} \tag{3}$$

where: $PSA(T_i)$ is the 5% damped pseudo spectral acceleration at T_i; and pga is the peak ground acceleration. In computing T_o, PSA are computed for oscillators having natural periods that are equally spaced on a log scale (i.e., $\Delta \log T_i$). Essentially, Equation 3 smoothes the normalized pseudo spectral acceleration response having an amplitude greater than or equal to 1.2. An example of a normalized pseudo acceleration spectrum, along with the minimum value of the normalized spectrum considered in the period determination, is shown in Figure 3.

Median Spectral Velocity-Acceleration Period ($T_{V/A50}$)

Shimazaki and Sozen (1984) initially proposed the definition of the spectral velocity-acceleration period ($T_{V/A50}$), which is given by:

$$T_{\text{V/A50}} = 2\pi \cdot \frac{pgv}{pga} \cdot \frac{\alpha_V(\xi = 5\%)}{\alpha_A(\xi = 5\%)} \tag{4}$$

where: pgv and pga are the peak ground velocity and acceleration, respectively, and are expressed in consistent units; α_V and α_A are the dimensionless median spectral amplification factors for 5% damping (i.e., $\xi = 5\%$). The α_V and α_A used herein are those proposed by Newmark and Hall (1982) and are equal to

1.65 and 2.12, respectively. $T_{V/A50}$ is the period corresponding to the intersection of the constant pseudo spectral acceleration (*PSA*) and constant pseudo spectral velocity (*PSV*) regions of the 5% damped Newmark-Hall design spectrum, where the design spectrum is constructed using the *pga*, *pgv*, and peak ground displacement (*pgd*) of a given earthquake motion. An example of a Newmark-Hall design spectrum is shown in Figure 4. Also shown in this figure is the response spectrum for the motion from which the *pga*, *pgv*, and *pgd* values were used to construct the Newmark-Hall spectrum.

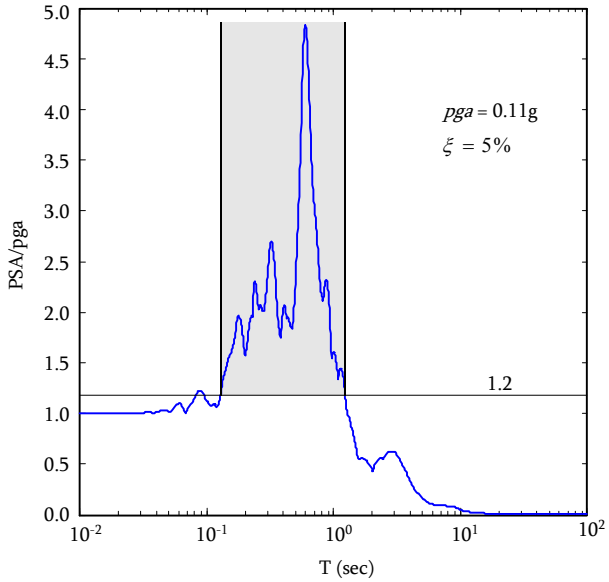

Figure 3. Example of normalized pseudo spectral acceleration spectrum (damping ratio ξ = 5%) and the range considered in computation of T_0 (shown in gray background) for an earthquake ground motion (Lee, 2009).

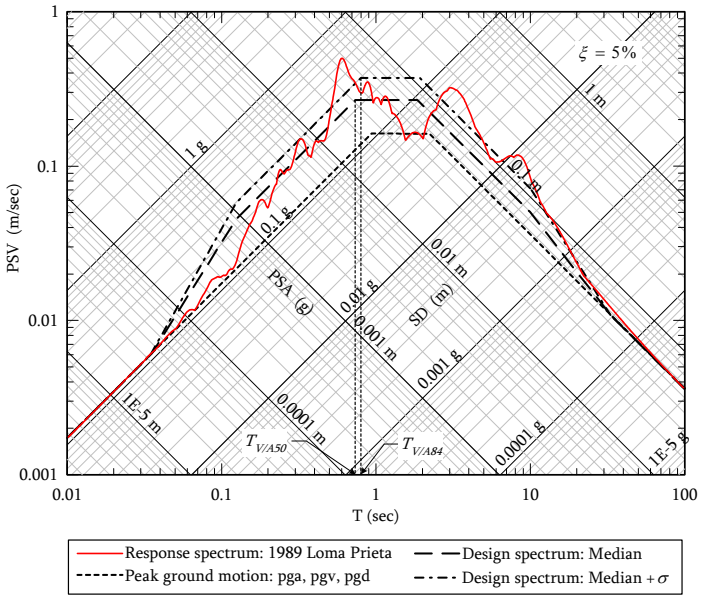

Figure 4. Example the Newmark-Hall design spectrum and corresponding response spectrum for an earthquake ground motion. Note that only $T_{V/A50}$ is examined in the study presented herein (Lee, 2009).

Peak Ground Velocity-Acceleration Period ($T_{v/a}$)

The peak ground velocity-acceleration period ($T_{v/a}$) is simply the ratio of *pgv* and *pga*, multiplied by 2π, where *pgv* and *pga* are expressed in consistent units. $T_{v/a}$ is given by:

$$T_{\text{v/a}} = 2\pi \cdot \frac{pgv}{pga} \tag{5}$$

EARTHQUAKE GROUND MOTIONS

Eleven acceleration time histories were used in the study presented herein. These time histories consisted of ten motions recorded during actual earthquakes ranging magnitude (M) and site-to-source distance (R). The eleventh motion was a windowed sine wave. The specific ground motions used and their characteristic periods are listed in Table1, where the magnitudes are moment magnitude and site-to-source distances are the closest distances to the fault rupture plane. All the motions are from active shallow crustal tectonic regimes and were recorded on rock sites.

Table 1. Acceleration time histories and characteristic periods

Earthquake	Station	M	R (km)	Characteristic Period (sec)				
				T_o	T_m	T_{avg}	$T_{V/A50}$	$T_{v/a}$
Coalinga	Oil City	5.8	8.2	0.215	0.305	0.359	0.243	0.312
N. Palm Springs	Murrieta Hot Springs	6.0	63.3	0.217	0.598	0.666	0.435	0.222
Gazli, USSR	Karakyr	6.8	3.0	0.179	0.419	0.652	0.498	0.639
Coalinga	Parkfield – Chrolame 2E	6.4	40.5	0.386	0.617	0.803	0.568	0.364
Parkfield	San Luis Obispo	6.1	60.0	0.270	0.422	0.591	0.365	0.234
Borrego Mtn	San Onofre – So Cal Edison	6.8	124.7	0.293	0.519	0.655	0.447	0.573
Landers	Lucerne	7.3	1.1	0.101	0.321	0.938	0.677	0.868
Duzce, Turkey	Sakarya	7.1	42.7	0.206	0.356	0.634	1.203	0.771
Landers	Riverside Airport	7.3	96.1	0.169	0.259	0.580	0.351	0.113
Tabas, Iran	Kashmar	7.4	199.1	0.622	0.916	1.120	1.521	0.488
windowed sine wave	T = 0.35 sec; *pga* = 0.3g	NA	NA	0.314	0.347	0.343	0.275	0.353

As may be observed from Table 1, the characteristic periods of a given motion can vary significantly. In fact, motions were specifically selected for this study such that this would be the case. The authors selected these ten recorded motions from a database containing over six hundred motions. Of the motions reviewed, approximately 30% had characteristic periods that were similar in value.

Space limitations preclude showing plots of all the acceleration time histories. However, the windowed sine wave is shown in Figure 5. The windowed sine wave has a period of 0.35 sec and 0.3g amplitude. The window function, shown in red in Figure 5, consists of 4 seconds of exponential rise time, 4 seconds of constant-amplitude strong motion, and 32 seconds of exponential decay, resulting in a motion having a 40-second total duration. This window function is similar to that proposed by Jennings et al. (1968). The motion was based-line corrected using a parabolic function.

SITE RESPONSE ANALYSES

The eleven acceleration time histories were used as input motions in a series of site response analyses. The analyses were performed using the computer code DeepSoil V3.7 (Hashash, 2009). The motions were propagated up through a 5% damped, linear elastic, single "soil" layer that overlaid a 1% damped elastic

half space. The motions were specified as rock outcrop motions at the surface of the elastic half space. The thickness of the soil layer was varied such that the ratio of the fundamental period (T_n) of the soil profile to the characteristic period of the ground motions ranged from about 0 to 4 (i.e., $0 \leq T_n/T_{char} \leq 4$, where T_{char} represents one of the five characteristic periods examined in this study). T_n is given by:

$$T_{\mathrm{n}} = \frac{4H}{V_s} \tag{6}$$

where: H and V_s are the thickness and shear wave velocity of the soil layer, respectively. In total, 19 different thicknesses of the soil layer were used in this study, with V_s for the layers equaling 305 m/sec (1000 ft/sec).

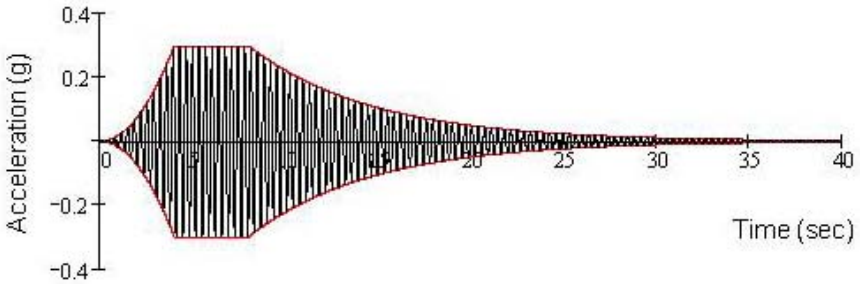

Figure 5. Windowed sine wave.

The normalized transfer function ($H(f)$) from rock outcrop to soil surface for the soil profiles is shown in Figure 6. The transfer function is normalized such that its peak (i.e., fundamental mode) occurs when frequency equals 1 Hz. By plotting the transfer function this way, it can be viewed as the ratio of *pga* at the soil surface to the *pga* at the rock outcrop ($pga_{soil\ surface}/pga_{rock\ outcrop}$) for an infinite duration sine wave, having period T_{char}, propagated up through the profile. To show this, the $pga_{soil\ surface}/pga_{rock\ outcrop}$ for the site response analyses using the windowed sine wave as the input motion are also plotted in Figure 6; in this plot, T_{char} was set to 0.35 sec, the known period of the windowed sine wave. As may be observed from this figure, the normalized transfer function and $pga_{soil\ surface}/pga_{rock\ outcrop}$ for the windowed sine wave are in excellent agreement. The slight differences between the two are attributed to the finite duration of the windowed sine wave, the base line correction applied to the time history, and the numerical errors associated with performing discrete fast Fourier and discrete inverse Fourier transforms inherent to the site response code.

Similar to Figure 6, the $pga_{soil\ surface}/pga_{rock\ outcrop}$ were computed for the ten earthquake motions, with T_{char} set equal to the corresponding values listed in Table 1. As an example, $pga_{soil\ surface}/pga_{rock\ outcrop}$ are plotted as a function of $T_n/T_{V/A50}$ in Figure 7 for the Coalinga earthquake, Oil City motion. As may be observed from this figure, the normalized transfer function and the $pga_{soil\ surface}/pga_{rock\ outcrop}$ are not in nearly as good of agreement as those for the windowed sine wave motion (i.e., Figure 6). However, common trends between the normalized transfer function and the $pga_{soil\ surface}/pga_{rock\ outcrop}$ are clearly identifiable in Figure 7. In the next section, a validation metric is proposed to quantify the goodness of the match between the normalized transfer function and the *pga* ratios.

VALIDATION METRIC

Validation of numerical codes and models that are used to predict physical processes is an evolving discipline (e.g., Oberkampf and Trucano, 2002; Schwer, 2007). Some of the concepts that are used to assess or rank the predictions by numerical models of various complex system responses in controlled experiments are borrowed herein. However, in this study, a comparison is being made between a numerical approximation and an analytical solution. Specifically, an assessment is being made regarding how well $pga_{soil\ surface}/pga_{rock\ outcrop}$ vs. T_n/T_{char} matches $H(f)$ for the different definitions of T_{char}. The basis for this comparison is that representing an earthquake ground motion by its characteristic period is similar in concept to representing an earthquake ground motion by a windowed sine wave having a period T_{char}.

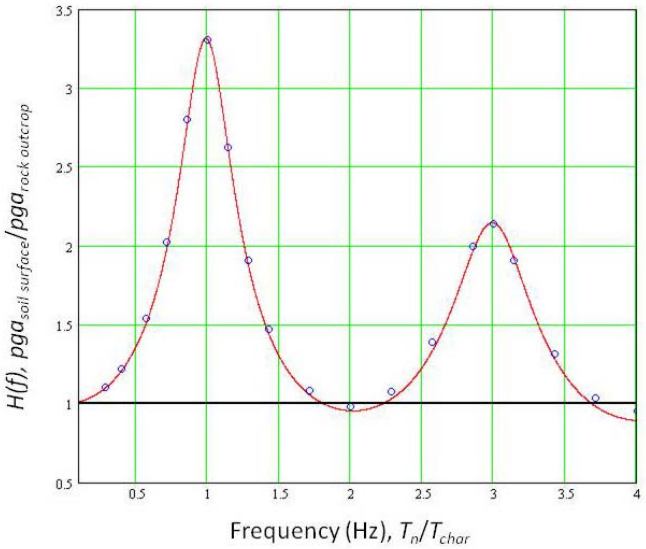

Figure 6. Normalized transfer function (red line) and amplification of windowed sine wave (blue circles).

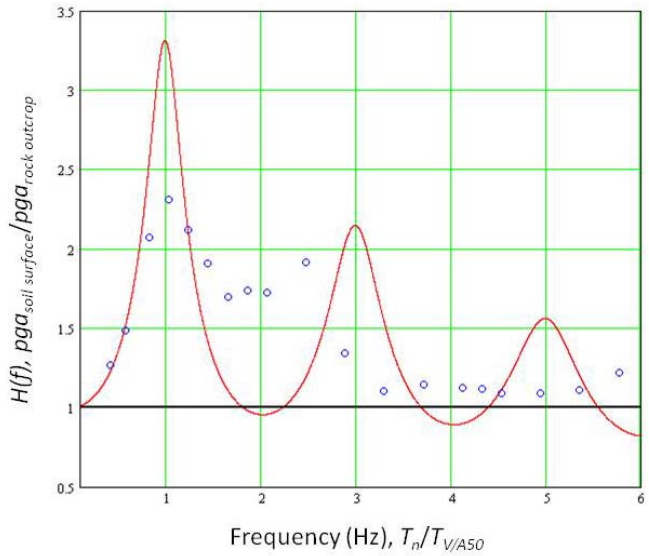

Figure 7. Normalized transfer function (red line) and amplification of the Coalinga earthquake, Oil City motion (blue circles).

The validation metric equation used in this study is a modification of the one proposed by Oberkampf and Trucano (2002). The equation is based on the relative error between the analytical and corresponding numerical predicted values and yields a number ranging from 0 to 1, with 0 indicating a very poor match between the analytical and predicted values and 1 indicating a perfect match. The validation metric equation is:

$$VM = 1 - \sum_{i=1}^{N} wf_i \cdot \tanh \left| \frac{y\left(\left(\frac{T_n}{T_{char}}\right)_i\right) - Y\left(\left(\frac{T_n}{T_{char}}\right)_i\right)}{Y\left(\left(\frac{T_n}{T_{char}}\right)_i\right)} \right| \tag{7a}$$

where: VM is the validation metric and ranges from 0 to 1; $y(\cdot)$ is the predicted value at $(T_n/T_{char})_i$ (i.e., $pga_{soil\ surface}/pga_{rock\ outcrop}$ at $(T_n/T_{char})_i$); $Y(\cdot)$ is the analytical value at $(T_n/T_{char})_i$ (i.e., $H(f)$ at $(T_n/T_{char})_i$); wf_i is a weighting factor that varies as a function of $(T_n/T_{char})_i$; and N is the total number of comparisons being made between the predicted and analytical values.

The wf_i used in this study is given by Equation 7b and is what makes Equation 7a differ from the VM equation proposed by Oberkampf and Trucano (2002). By adjusting the value of n in Equation 7b, the weight applied to the relative differences between the predicted and analytical values can be varied as a function of T_n/T_{char}. The desire for this is that, depending on the application, different modes of vibration will have different levels of importance. For example, the permanent relative displacement of retaining walls subjected to earthquake excitations is almost completely controlled by first mode response. As a result, higher weights should be placed on the relative difference between the predicted and analytical values for T_n/T_{char} less than around 1, with the differences between the predicted and analytical values for T_n/T_{char} greater than about 2 having almost no importance. This can be achieved in Equation 7b by setting n equal to 1. In contrast, for site response analyses, higher modes may be of importance, although the first few modes are certainly the more important than the later modes. Accordingly, setting n equal to 5 can capture this relative importance of the modes to the overall response. Plots of wf for n equal to 1 and 5 are shown in Figure 8. In the limit, as n gets large, $wf \approx 1/N$ (i.e., the relative differences between the predicted and analytical values are equally weighted, independent of T_n/T_{char}). In this case, Equation 7a reduces to the VM equation proposed by Oberkampf and Trucano (2002).

$$wf_i = \frac{\exp\left[-\frac{1}{n} \cdot \left(\frac{T_n}{T_{char}}\right)_i\right]}{\sum_{i=1}^{N} \exp\left[-\frac{1}{n} \cdot \left(\frac{T_n}{T_{char}}\right)_i\right]} \tag{7b}$$

Using Equation 7a and 7b, the VM for both site response analyses (n = 5) and retaining wall analyses (n = 1) were computed for the ten earthquake ground motions. The resulting values are listed in Table 2. The relative influence of the wf can be understood by looking at the VM for $T_{V/A50}$ for the Coalinga earthquake, Oil City motion, the numerical and analytical values for which are plotted in Figure 7. From Table 2, the VM are 0.730 and 0.795 for site response and retaining wall analyses, respectively. The higher VM for retaining walls, as compared to the VM for site response analyses, implies that the numerical results captured the first mode response better than higher modes, which may also be observed in Figure 7.

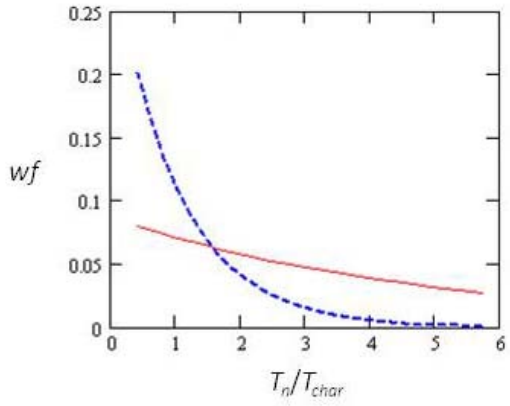

Figure 8. Weighting function (*wf*) for site response analyses (solid, red line: $n = 5$) and retaining walls (dashed, blue line: $n = 1$) for $N = 19$.

Table 2. Validation metrics for site response and retaining wall analyses

Earthquake	Station	M	R (km)	Validation Metric*				
				T_o	T_m	T_{avg}	$T_{V/A50}$	$T_{v/a}$
Coalinga	Oil City	5.8	8.2	0.709/ 0.748	0.761/ 0.789	0.724/ 0.737	0.730/ 0.795	0.752/ 0.783
N. Palm Springs	Murrieta Hot Springs	6.0	63.3	0.765/ 0.761	0.625/ 0.597	0.613/ 0.598	0.638/ 0.613	0.761/ 0.756
Gazli, USSR	Karakyr	6.8	3.0	0.756/ 0.782	0.717/ 0675	0.733/ 0.703	0.775/ 0.714	0.738/ 0.706
Coalinga	Parkfield – Chrolame 2E	6.4	40.5	0.684/ 0.701	0.711/ 0.714	0.710/ 0.685	0.689/ 0.696	0.677/ 0.704
Parkfield	San Luis Obispo	6.1	60.0	0.704/ 0.660	0.687/ 0.647	0.703/ 0.656	0.677/ 0.641	0.699/ 0.683
Borrego Mtn	San Onofre – So Cal Edison	6.8	124.7	0.754/ 0.793	0.734/ 0.716	0.697/ 0.663	0.754/ 0.754	0.721/ 0.694
Landers	Lucerne	7.3	1.1	0.703/ 0.659	0.736/ 0.720	0.598/ 0.605	0.679/ 0.643	0.609/ 0.608
Duzce, Turkey	Sakarya	7.1	42.7	0.661/ 0623	0.661/ 0.591	0.679/ 0.595	0.531/ 0.512	0.629/ 0.566
Landers	Riverside Airport	7.3	96.1	0.660/ 0.622	0.794/ 0.757	0.662/ 0.570	0.681/ 0.643	0.616/ 0.608
Tabas, Iran	Kashmar	7.4	199.1	0.679/ 0.720	0.640/ 0.622	0.576/ 0.562	0.574/ 0.552	0.675/ 0.733
Average				0.708/ 0.707	0.707/ 0.683	0.670/ 0.637	0.673/ 0.656	0.688/ 0.684

*The top number is the VM for site response analyses ($n = 5$) and the lower number is for retaining wall response ($n = 1$).

DISCUSSION

The average *VM* for the ten earthquake ground motions for each characteristic period definition is given in the last row of Table 2. These values can be compared to determine which definition(s) are most appropriate for selecting ground motions for analyzing the dynamic response of soil profiles and retaining walls. T_o has the highest *VM* for both site response and retaining wall analyses, and thus is the most

appropriate definition for characteristic period for motions used in site response and retaining wall analyses.

As may be observed from Table 2, the range in the average *VM* for all the characteristic period definitions is small, ranging from a low of 0.637 to a high of 0.708. This actually implies that all the characteristic period definitions are moderate-to-poor in their ability to represent the frequency content of earthquake motions (it should not come as a big surprise that representing an earthquake motion by a single period is tenuous). Given this finding, the peak ground velocity-acceleration period ($T_{v/a}$) may be worth further consideration for wider use, mainly because it is the simplest of all the characteristic periods to calculate.

SUMMARY AND CONCLUSIONS

In this study, five commonly used definitions of characteristic period were examined: the mean period (T_m); the average spectral period (T_{avg}); the smoothed spectral period (T_o); the median spectral velocity-acceleration period ($T_{V/A50}$); and the peak ground velocity-acceleration period ($T_{v/a}$). The characteristic period definitions were assessed by computing the amplification of earthquake ground motions propagated up through shallow soil profiles (e.g., backfill of retaining walls) and deeper soil profiles. These results were compared to the analytical solution of sinusoidal motions propagated up through the same soil profiles, where the periods of the sinusoidal motions equaled the characteristic periods of the earthquake ground motions. A validation metric was used to determine which characteristic period definition is most suitable for site response and retaining wall analyses. The results showed that characterizing an earthquake ground motion by a single period, regardless of how quantified, is tenuous. However, of the definitions examined, T_o is the most suitable definition for motions used in the dynamic response of both soil profiles and retaining wall.

ACKNOWLEDGEMENTS

This material is based upon work supported, in part, by the National Science Foundation under Grant No. CMMI 0644580. This support is gratefully acknowledged. However, any opinions, findings, and conclusions or recommendations expressed in this material are those of the authors and do not necessarily reflect the views of the National Science Foundation.

REFERENCES

Blake, T.F., Hollingsworth, R.A., and Stewart, J.P. (2002). Recommended Procedures for Implementation of DMG Special Publication 117: Guidelines for Analyzing and Mitigating Landslide Hazards in California, Southern California Earthquake Center, Los Angeles, CA.

Green, R.A. and Cameron, W.I. (2003). "The Influence of Ground Motion Characteristics on Site Response Coefficients," Proc., 7th Pacific Conference on Earthquake Engineering, University of Canterbury, Christchurch, New Zealand, Feb. 13-15, Paper Number 90, 8pp.

Green, R.A., Olgun, C.G., and Wissmann, K.J. (2008). "Shear Stress Redistribution as a Mechanism to Mitigate the Risk of Liquefaction," Geotechnical Earthquake Engineering and Soil Dynamics IV (David Zeng, Majid T. Manzari, and Dennis R. Hiltunen, eds.), ASCE Geotechnical Special Publication 181.

Goughnour, R.R. and Pestana, J.M. (1998). "Mechanical Behavior of Stone Columns Under Seismic Loading," Proc. 2nd International Conference on Ground Improvement Techniques, Singapore.

Hashash, Y.M.A. (2009). DeepSoil V3.7, Department of Civil and Environmental Engineering, University of Illinois at Urbana Champaign.

Jennings, P.C., Housner, G.W., and Tsai, N.C. (1968). Simulated Earthquake Motions, EERL 1968.004, California Institute of Technology, Pasadena, CA.

Lee, J. (2009). Engineering Characterization of Earthquake Ground Motions, Ph.D. Dissertation, Department of Civil and Environmental Engineering, University of Michigan, Ann Arbor, MI, USA, 246p

Newmark, N.M and Hall, W.J. (1982). Earthquake Spectra and Design, Monograph MNO-3, Earthquake Engineering Research Institute, Oakland, CA.

Oberkampf, W.L. and Trucano, T.G. (2002). "Verification and Validation in Computational Fluid Dynamics," Progress in Aerospace Sciences, 38, 209-272.

Rathje, E.M., Faraj, F., Russell, S., and Bray, J.D. (2004). "Empirical Relationships for Frequency Content Parameters of Earthquake Ground Motions," Earthquake Spectral, 20(1), 119-144.

Rathje, E.M., Abrahamson, N.A., and Bray, J.D. (1998). "Simplified Frequency Content Estimates of Earthquake Ground Motions," Journal of Geotechnical and Geoenvironmental Engineering, 124(2), 150-159.

Schwer, L.E. (2007). "Validation Metrics for Response Histories: Perspectives and Case Studies," Engineering with Computers, 23, 295-309.

Shimazaki, K. and Sozen, M.A. (1984). Seismic Drift of Reinforced Concrete Structures. Special Research Paper (Draft). Hazama Corp.

Stewart, J.P., Chiou, S.-J., Bray, J.D., Somerville, P.G., Graves, R.W., and Abrahamson, N.A. (2001). Ground Motion Evaluation Procedures for Performance Based Design, Report No. PEER-2001/09, Pacific Earthquake Engineering Research Center, September, 229pp.

Stewart, J.P., Blake, T.M., and Hollingsworth, R.A. (2003). "A Screen Analysis Procedure for Seismic Slope Stability," Earthquake Spectra, 19(3), 697-712.